Severe lung fibrosis requires an invasive fibroblast phenotype regulated by hyaluronan and CD44

Yuejuan Li,[1] Dianhua Jiang,[1] Jiurong Liang,[1] Eric B. Meltzer,[1] Alice Gray,[1] Riu Miura,[2] Lise Wogensen,[3] Yu Yamaguchi,[2] and Paul W. Noble[1]

[1]Division of Pulmonary, Allergy, and Critical Care Medicine, Department of Medicine, Duke University School of Medicine, Durham, NC 27710
[2]Sanford Children's Health Research Center, Burnham Institute for Medical Research, La Jolla, CA 92037
[3]Research Laboratory for Biochemical Pathology, Aarhus University Hospital, DK-8000 Aarhus, Denmark

Tissue fibrosis is a major cause of morbidity, and idiopathic pulmonary fibrosis (IPF) is a terminal illness characterized by unremitting matrix deposition in the lung. The mechanisms that control progressive fibrosis are unknown. Myofibroblasts accumulate at sites of tissue remodeling and produce extracellular matrix components such as collagen and hyaluronan (HA) that ultimately compromise organ function. We found that targeted overexpression of HAS2 (HA synthase 2) by myofibroblasts produced an aggressive phenotype leading to severe lung fibrosis and death after bleomycin–induced injury. Fibroblasts isolated from transgenic mice overexpressing HAS2 showed a greater capacity to invade matrix. Conditional deletion of HAS2 in mesenchymal cells abrogated the invasive fibroblast phenotype, impeded myofibroblast accumulation, and inhibited the development of lung fibrosis. Both the invasive phenotype and the progressive fibrosis were inhibited in the absence of CD44. Treatment with a blocking antibody to CD44 reduced lung fibrosis in mice in vivo. Finally, fibroblasts isolated from patients with IPF exhibited an invasive phenotype that was also dependent on HAS2 and CD44. Understanding the mechanisms leading to an invasive fibroblast phenotype could lead to novel approaches to the treatment of disorders characterized by severe tissue fibrosis.

CORRESPONDENCE
Paul W. Noble:
paul.noble@duke.edu

Abbreviations used: ASMA, α–smooth muscle actin; BAL, bronchoalveolar lavage; BALF, BAL fluid; HA, hyaluronan; HABP, HA-binding protein; IPF, idiopathic pulmonary fibrosis; MMP, matrix metalloproteinase; mRNA, messenger RNA; qRT-PCR, quantitative RT-PCR; siRNA, small interfering RNA; TIMP, tissue inhibitor of metalloproteinase.

Progressive tissue fibrosis is a major cause of morbidity and mortality. Although numerous mediators have been identified as initiating tissue fibrosis, the mechanisms that contribute to persistent fibrodestructive disease remain incompletely understood. Fibroblasts are critical effector cells in mediating tissue remodeling. At sites of tissue injury and remodeling, there is also the accumulation of myofibroblasts, and their origins remain a source of active investigation (Hinz et al., 2007). Myofibroblasts are important sources of matrix production and also have contractile properties critical for wound healing (Blankesteijn et al., 1997). One of the defining characteristics of myofibroblasts is the expression of α–smooth muscle actin (ASMA). Intratracheal administration of bleomycin has been widely used as a model to study the mechanisms of noninfectious

injury and repair in the lung. Myofibroblasts are recruited to the lung interstitium 7–14 d after bleomycin injury and dissipate through apoptosis by 21 d (Zhang et al., 1996). Although considerable evidence has accumulated defining mediators such as TGF-β that are essential for fibroblasts to express ASMA and assume contractile functions (Kim et al., 2009), there has been no in vivo demonstration that controlling ASMA-expressing cells regulates chronic tissue fibrosis.

Idiopathic pulmonary fibrosis (IPF) is a terminal illness characterized by progressive and unremitting matrix deposition in the interstitium of the lung (Bjoraker et al., 1998). The clinical course of IPF is unrelenting and reminiscent of cancer with patients suffocating

R. Miura's present address is Evec, Inc. Sapporo Laboratory, Sapporo 060-0004, Japan.

from the inexorable accumulation of extracellular matrix in the gas-exchanging regions of the lung. A hallmark and defining pathological feature of IPF is the formation of fibroblastic foci, which are the accumulation of myofibroblasts in the interstitium of the lung juxtaposed to the alveolar epithelium with destruction of the adjoining alveolar basement membrane (Selman and Pardo, 2002). The destruction of alveolar basement membrane was also observed in experimental lung fibrosis (Fukuda et al., 1985; Vaccaro et al., 1985). Fibroblasts and myofibroblasts from IPF patients have been shown to have distinct properties (Larsson et al., 2008), including the ability to invade extracellular matrix in the manner of metastatic cancer cells (White et al., 2003a).

Hyaluronan (HA) is a nonsulfated glycosaminoglycan produced by mesenchymal cells and a variety of tumor cells and has been suggested to contribute to tumor metastasis through interactions with its cognate cell surface receptor CD44 (Arch et al., 1992; Toole, 2004). Accumulation of HA has been shown to be a characteristic of disorders that are associated with progressive tissue fibrosis (Bjermer et al., 1989). HA has also been shown to accumulate in the lung after bleomycin treatment and has a role in regulating the inflammatory response (Jiang et al., 2005, 2011). Three HA synthase genes (*HAS1–3*) have been identified. Targeted deletion of *HAS2* generates an embryonic lethal phenotype

caused by impaired cardiac development (Camenisch et al., 2000). CD44 is the major cell surface receptor for HA and plays an important role in inflammatory cell recruitment (Mikecz et al., 1995; Siegelman et al., 1999) and activation (Noble et al., 1993; DeGrendele et al., 1997), as well as tumor growth and metastasis (Lesley et al., 1993). We have previously shown that CD44 is necessary for hematopoietic cells to clear HA from sites of inflammation (Teder et al., 2002). CD44 has been shown to be critical for the recruitment of fibroblasts to the injury sites (Acharya et al., 2008). The role of CD44 in fibrogenesis has not been directly addressed.

The inexorable course of progressive fibrosis in IPF led us to postulate that fibroblasts may take on properties similar to metastatic cancer cells that overexpress HA. Consistent with this concept is a recent study showing that IPF fibroblasts have abnormalities in translational control (Larsson et al., 2008) that can be found in cancer cells. One of the seminal properties of metastatic cancer cells is the ability to invade basement membrane. We reasoned that fibrotic fibroblasts and myofibroblasts drive fibrogenesis by invasion and destruction of basement membrane and that HA–CD44 interactions may regulate this process. We investigated the hypothesis that fibrotic fibroblasts acquire an invasive phenotype that is essential for progressive fibrogenesis and that HA and CD44 have critical roles in regulating the process.
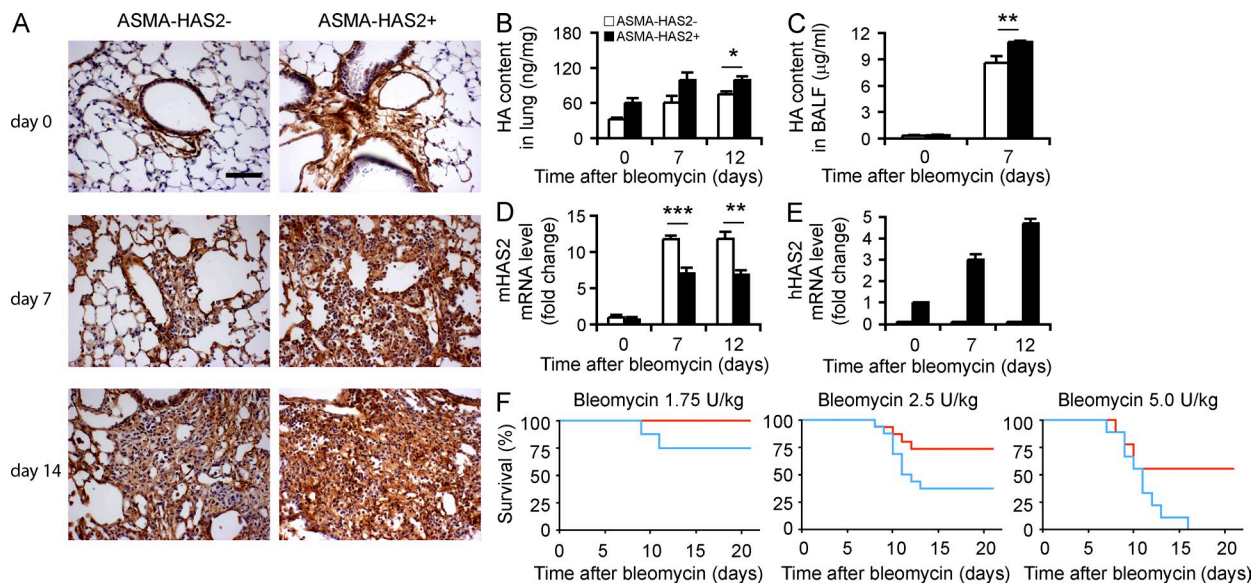

Figure 1. **ASMA–HAS2 transgenic mice accumulate HA and show increased mortality after bleomycin challenge.** (A) Distribution of HA in lungs of ASMA-HAS2+ and littermate control mice (ASMA-HAS2−) was determined by immunohistochemical staining of HA with biotin-HABP. Representative sections from five bleomycin-treated samples and three controls are shown. The specificity of the staining was determined by preincubating tissue samples with 10 U/ml streptomyces hyaluronidase for 2 h at room temperature (not depicted). Bar, 50 µm. (B and C) HA concentration in lung tissue (B) and BALF (C) from ASMA-HAS2+ mice and control mice (ASMA-HAS2−) at different times after bleomycin treatment ($n = 5$–7; *, $P < 0.05$; **, $P < 0.01$). (D and E) Murine HAS2 (mHAS2; D and E) and human HAS2 (hHAS2; E) mRNA expression levels in ASMA-HAS2+ mice and controls (ASMA-HAS2−) at various time points after bleomycin treatment were measured using real-time PCR ($n = 3$–5; **, $P < 0.01$; ***, $P < 0.001$). (B–E) Error bars indicate mean ± SEM. (F) ASMA-HAS2+ and control mouse lung injury was induced after intratracheal inoculation with the indicated dose of bleomycin. Percentages of surviving mice were plotted over a 21-d period (for 1.75 U/kg: $n = 8$ per group, $P = 0.14$; for 2.5 U/kg: $n = 16$ per group, $P = 0.05$; for 5.0 U/kg: $n = 9$ per group, $P < 0.05$; red line, ASMA-HAS2−; blue line, ASMA-HAS2+). (A–F) Experiments were performed three times.

RESULTS

Targeted overexpression of HAS2 in ASMA–expressing cells generates a severe fibrotic phenotype

To characterize the role of HAS2 expression by myofibroblasts in the pathogenesis of pulmonary fibrosis, we evaluated transgenic mice with targeted human HAS2 expression in ASMA-expressing cells (Chai et al., 2005). ASMA-HAS2 transgenic mice develop normally and exhibit no overt phenotype in the unchallenged state. Intratracheal administration of bleomycin recruits myofibroblasts (Zhang et al., 1996) and causes pulmonary fibrosis. ASMA-HAS2 transgenic mice exhibited an increase in HA deposition around large airways and blood vessels at baseline and accumulate increased concentrations of HA in both the lung interstitium and alveolar space after injury (Fig. 1, A–C). Endogenous murine *HAS2* gene expression was upregulated after bleomycin treatment (Fig. 1 D), but human *HAS2* was only expressed in the transgenic mice (Fig. 1 E). ASMA-HAS2 transgenic mice demonstrated a marked increase in mortality after lung injury over a dose range of bleomycin (Fig. 1 F). To evaluate the mechanisms leading to increased mortality in ASMA-HAS2 transgenic mice, we first examined the inflammatory response after lung injury. ASMA-HAS2 transgenic mice were found to have an increase in total inflammatory cells relative to transgene negative controls, and the increase was largely the result of an influx of neutrophils (Fig. S1, A–C). We analyzed the bronchoalveolar lavage (BAL) fluid (BALF) for neutrophil chemotactic peptides and found a significant increase in the chemokine KC in the ASMA-HAS2 transgenic mice (Fig. S1 D). It has previously been shown that HA fragments accumulate after lung injury and stimulate macrophages to produce inflammatory mediators (McKee et al., 1996). ASMA-HAS2 transgenic mice were found to accumulate abundant HA fragments in lung tissue (Fig. S2, A and B).

We then examined the fibrotic response in ASMA-HAS2 transgenic mice and found evidence of progressive fibrosis at time points (28 d) when the fibrotic response in transgene-negative mice was abating (Fig. 2, A and B). Both the magnitude and duration of the fibrotic response were greater in the ASMA-HAS2 transgenic mice. Furthermore, a fibrodestructive response in the periphery of the lung was observed in the ASMA-HAS2 transgenic mice (Fig. 2 A) similar to that observed in lung tissue from patients with IPF. We also found an impressive increase in the accumulation of ASMA staining in lung tissue from ASMA-HAS2 transgenic mice consistent with greater accumulation of myofibroblasts (Fig. 2, C and D), which is similar to what is observed in IPF lung tissue (Fig. 2 E).

Conditional knockout of HAS2 in mesenchymal cells diminishes the accumulation of myofibroblasts and the development of pulmonary fibrosis

HAS2-deficient mice have an embryonic lethal phenotype (Camenisch et al., 2000). To ascertain the role of HA in mesenchymal cell functions, we generated *Has2^flox/+* mice (Matsumoto et al., 2009) and crossed them with a Col1α2–iCre transgenic line (Florin et al., 2004). Unfortunately, the vast majority of Col1α2-iCre+/*Has2^flox/flox* mice (*Has2^CKO/CKO*) also die in utero, suggesting that HA production by mesenchymal cells drives the phenotype. We were able to perform bleomycin experiments with nine surviving mice obtained over the years from extensive breeding. Conditional *Has2^CKO/CKO* mice were treated with bleomycin at 8 wk of age. Our preliminary data showed that *Has2^CKO/CKO* mice had minimal HA staining in bronchial tissues at baseline and developed significantly less fibrosis after lung injury as estimated by trichrome staining (Fig. S3, A and B).
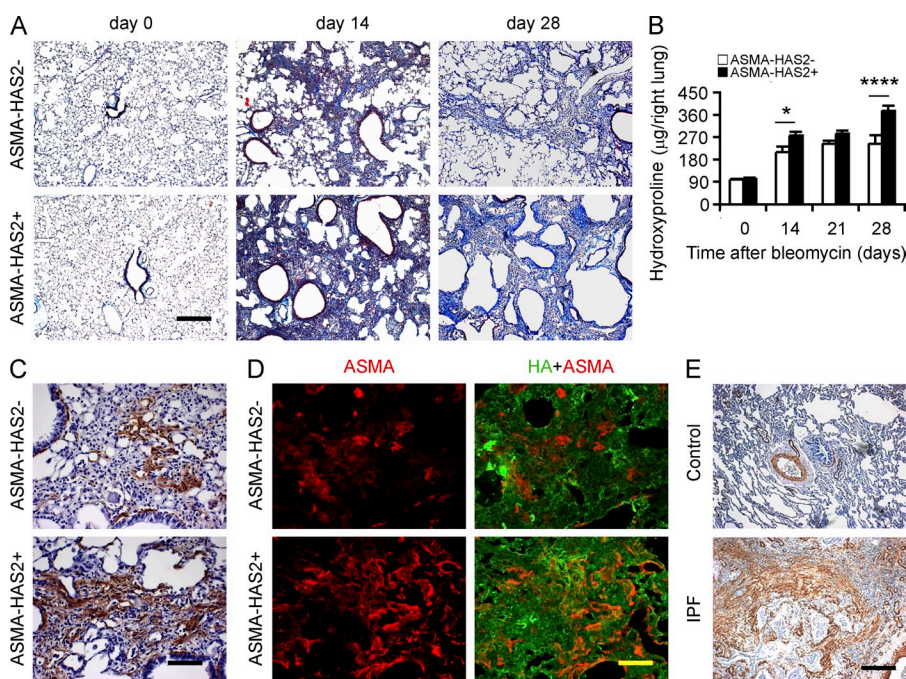

Figure 2. ASMA–HAS2 transgenic mice exhibit increased collagen content in lungs after bleomycin treatment. (A) Lung sections of ASMA-HAS2+ and transgene negative controls 0, 14, and 28 d after bleomycin instillation were stained using Masson's trichrome method. Representative images of the staining are shown (*n* = 6–7). (B) Lung tissues from ASMA-HAS2+ and controls on days 0, 14, 21, and 28 after bleomycin treatment were collected and assayed for collagen content using the hydroxyproline method (*n* = 6–7 per group; *, P < 0.05; ****, P < 0.0001). The experiments were performed three times. Error bars indicate mean ± SEM. (C and D) Immunohistochemical (C) and immunofluorescent analysis (D) of ASMA and HA in lung sections of ASMA-HAS2+ and control mice 14 d after bleomycin treatment. Representative images of the staining are shown (*n* = 6–7). (C) DAB staining is shown. (D) Immunofluorescence staining is shown. (E) Representative images of IPF patients' and control lung tissues showing ASMA staining and similar fibrotic changes to bleomycin-induced lung fibrosis. Bars: (A and E) 200 µm; (C and D) 50 µm.

In addition, at sites of lung remodeling, there was a marked reduction in myofibroblast accumulation in the lung relative to WT or ASMA-HA transgenic mice (Fig. S3 C). To further assess the contribution of fibroblast expression of HAS2, we used an additional Cre line using the FSP-1 promoter. FSP-1 is expressed by lung fibroblasts (Lawson et al., 2005; Tanjore et al., 2009). FSP-1–Cre mice were crossed with the *Has2^{flox/flox}* line to generate FSP-1–Cre^+/*Has2^{flox/flox}* (*Has2^{FKO/FKO}*) mice. These mice are viable and demonstrate no overt phenotype in the unchallenged state. We challenged *Has2^{FKO/FKO}* mice with bleomycin and found a substantial inhibition in the accumulation of both HA (Fig. 3 A) and collagen in lung tissue after injury (Fig. 3, B and C). In addition, there was also a decrease in the accumulation of myofibroblasts as assessed by ASMA staining of lung tissues (Fig. 3 D). Thus, two different fibroblast driver lines show that HAS2 expression by mesenchymal cells is critical for the development of pulmonary fibrosis and myofibroblast accumulation after tissue injury. These gain and loss of function interventions support a fundamental role for HAS2 in the development of pulmonary fibrosis.

HAS2 expression in myofibroblasts promotes an invasive phenotype

We investigated the hypothesis that fibrotic fibroblasts acquire an invasive phenotype that is essential for severe fibrogenesis and that HAS2 is critical in regulating the process. We used an assay system in which fibroblasts are evaluated for their ability to spontaneously invade Matrigel, a composite matrix with basement membrane constituents. This assay has been used to analyze the metastatic potential of cancer cells (Qian et al., 1994; Karnoub et al., 2007). We compared fibroblasts isolated from ASMA-HAS2 transgenic mice and littermate control mice before and after bleomycin challenge. We found that fibrotic fibroblasts spontaneously invaded Matrigel (Fig. 4 A). Interestingly, invasive fibroblasts demonstrated increased HAS2 messenger RNA (mRNA) expression relative to fibroblasts isolated that did not invade matrix (Fig. 4 B), suggesting that *Has2* expression is an important feature of the subset of fibroblasts that invade matrix. Fibroblasts isolated from bleomycin-treated ASMA-HAS2 transgenic mice demonstrated greater invasive capacity than transgene-negative controls (Fig. 4 A). To determine the contribution of HA to the invasive phenotype, we sought to identify fibroblasts deficient in HAS2 expression and HA production. We were able to isolate fibroblasts from *Has2^{CKO/CKO}* and *Has2^{FKO/FKO}* mice and examined HA production. A hallmark of mesenchymal cell HA expression is the formation of cell surface HA coats (Spicer et al., 1996). HA is synthesized in the cell membrane and extruded to the external milieu (Itano et al., 1999). Conditional *Has2*-null (*Has2^{CKO/CKO}*) fibroblasts showed a marked reduction in
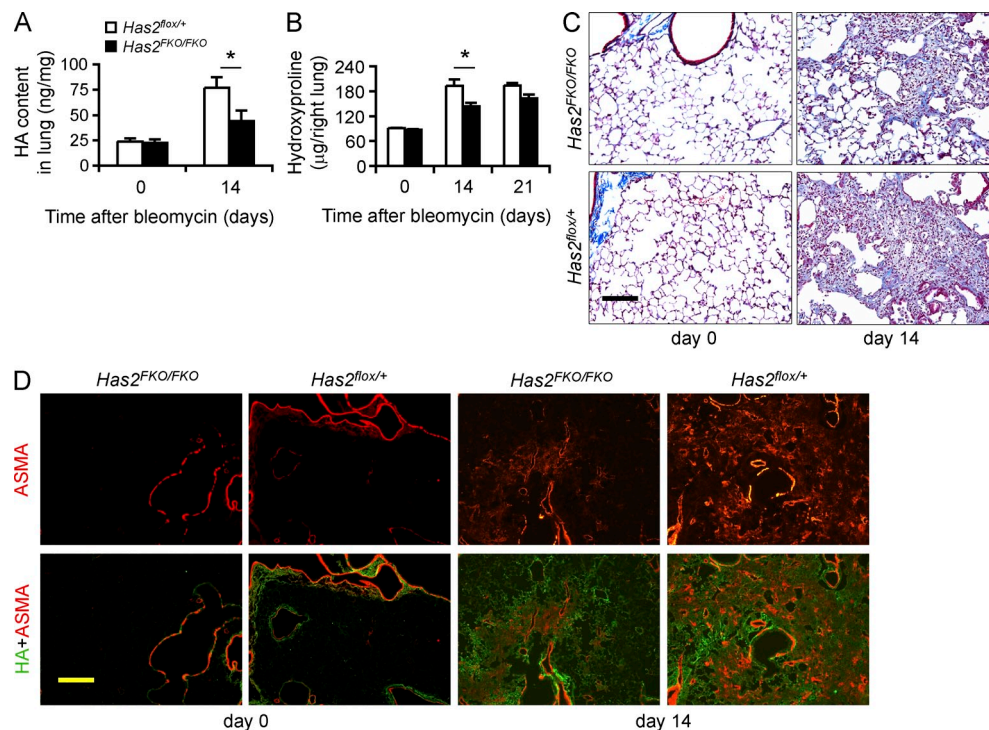

Figure 3. Targeted deletion of HAS2 in mesenchymal cells inhibits lung fibrosis and myofibroblast accumulation. (A) HA content in lung tissue from *Has2^{FKO/FKO}* and *Has2^{flox/+}* mice on day 14 after bleomycin treatment (n = 3–8 per group; *, P < 0.05). (B) Lung tissues from *Has2^{FKO/FKO}* and control *Has2^{flox/+}* mice on days 0, 14, and 21 after bleomycin treatment were collected and assayed for collagen content using the hydroxyproline method (n = 4–11 per group; *, P < 0.05). (A and B) Error bars indicate mean ± SEM. (C) Lung sections of *Has2^{FKO/FKO}* and *Has2^{flox/+}* mice on days 0 and 14 after bleomycin instillation were stained using Masson's trichrome method and counterstained with hematoxylin (n = 8 in each group). (D) Double staining of HA and ASMA in bleomycin-treated *Has2^{FKO/FKO}* and control *Has2^{flox/+}* mouse lung sections on days 0 and 14 after bleomycin instillation. The experiments were performed three times. Bars, 200 μm.

the ability to form cell surface coats and exclude exogenous particles (Fig. 4, C and D). Importantly, they were severely deficient in HA production (Fig. 4 E). We examined the ability of conditional *Has2*-null fibroblasts to invade Matrigel and

Figure 4. Fibroblast invasive capacity is dependent on HAS2.
(A) The spontaneous Matrigel-invading capacity of fibroblasts from bleomycin-treated (10 d) and saline-treated ASMA-HAS2+ and littermate control mice lungs was determined. Data are shown as the index of invasion value of the fibroblasts with or without bleomycin treatment over littermate control fibroblasts without bleomycin challenge (*n* = 4 per group; *, P < 0.05). (B) mRNA relative levels of HAS2 in invasive and noninvasive fibroblasts isolated from bleomycin-treated (11 d) WT mouse lungs were determined using real-time PCR (*n* = 5; *, P < 0.05). (C) Phase-contrast photomicrographs of the pericellular matrices (HA coat) in *Has2CKO/CKO* fibroblasts compared with those in *Has2flox/+* fibroblasts. Bar, 50 µm. (A–C) Experiments were performed three times. (D) Relative thickness of HA coat was calculated in 20 randomly selected cells using ImageJ (*n* = 10; ***, P < 0.001). Data represent one of two independent experiments. (E) HA content in cultured media of *Has2flox/+* and *Has2CKO/CKO* fibroblasts was measured using the HA-ELISA assay (*n* = 3; **, P < 0.01). The experiments were performed three times. (F) Comparison of the invasive capacity between *Has2flox/+* and *Has2CKO/CKO* fibroblasts. Data are shown as the invasion index of *Has2CKO/CKO* fibroblasts over *Has2flox/+* fibroblasts. They are representative of three independent experiments (*n* = 3; **, P < 0.01). (G) Comparison of the invasive capacity between fibroblasts from bleomycin-treated *Has2flox/+* and *Has2FKO/FKO* mice. Data are shown as the invasion index of *Has2FKO/FKO* fibroblasts over *Has2flox/+* fibroblasts (*n* = 3; *, P < 0.05). The experiments were performed three times. (A, B, and D–G) Error bars indicate mean ± SEM.

found a marked reduction in invasive capacity (Fig. 4, F and G). These gain and loss of function interventions support a fundamental role for HAS2 in the development of an invasive myofibroblast phenotype.
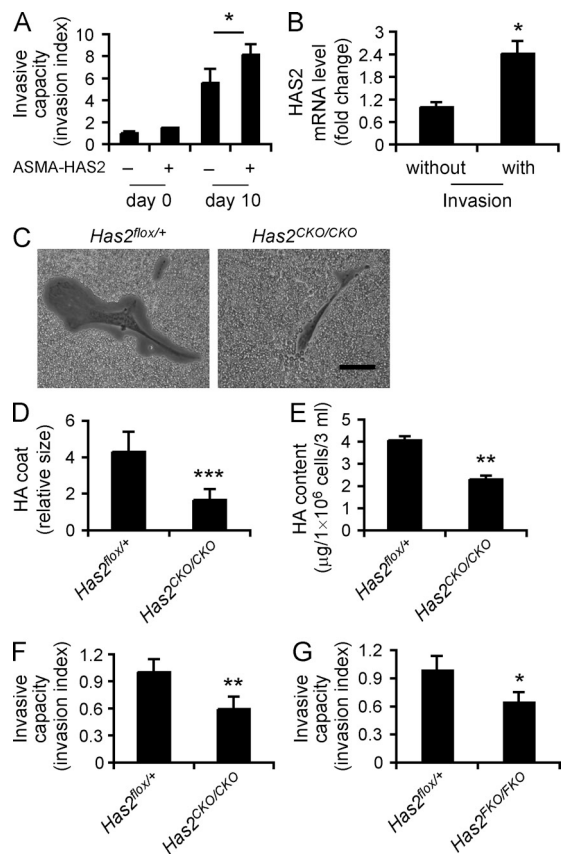
Deficiency of CD44 inhibits the progression of pulmonary fibrosis and regulates fibroblast/myofibroblast invasion of extracellular matrix

The cell surface adhesion molecule CD44 is a HA receptor, and macrophage CD44 is important for clearing HA fragments from injured lung tissue (Miyake et al., 1990; Teder et al., 2002). We found that CD44 was up-regulated after bleomycin-induced lung injury (Fig. 5, A and B) and to a greater extent in ASMA-HAS2 transgenic mice (Fig. 5 B). We evaluated the role of CD44 in mediating the fibrogenic response in several ways. CD44-null mice did not show significant protection from the development of pulmonary fibrosis (Fig. 5, C and D), but the effect was more pronounced when the ASMA-HAS2 transgenic mice were bred with the CD44-null mice (Fig. 5 E). We then administered systemic anti-CD44 blocking antibodies or an isotype-matched control at the time of lung injury. We found that lung collagen accumulation was significantly prevented in the ASMA-HAS2 transgenic mice in the presence of anti–CD44 antibodies (Fig. 5 F). To determine whether blocking CD44 could be of therapeutic benefit, we treated ASMA-HAS2 transgenic mice with systemic anti-CD44 antibodies or isotype-matched control on days 7, 14, and 21 after the bleomycin treatment and analyzed collagen content at day 28. Collagen content was significantly reduced in the presence of CD44 inhibition (Fig. 5, G and H).

To determine the role of CD44 in fibroblast invasion, we examined the invasive capacity of fibroblasts isolated from CD44-null mice after bleomycin treatment and found impaired invasive capacity (Fig. 5 I). Similar results were found from fibroblasts isolated from ASMA-HAS2+/CD44−/− mice relative to control mice (Fig. 5 J). Furthermore, treating fibroblasts isolated from bleomycin-challenged WT C57BL/6J mice with anti-CD44 antibodies blunted fibroblast invasion (Fig. 5 K).

HAS2 and CD44 regulate human IPF fibroblast invasion

To determine whether these data obtained from mouse models of fibrosis are relevant to human lung fibrosis, we isolated primary lung fibroblasts from patients with IPF and analyzed their invasive capacity. We found a striking increase in the invasive capacity of IPF fibroblasts compared with fibroblasts isolated from normal lung tissue (Fig. 6, A and B). These data suggest that fibroblasts from patients with progressive pulmonary fibrosis acquire an invasive phenotype, as previously described (Thannickal et al., 2003). Interestingly, HAS2 mRNA expression was increased in IPF fibroblasts that invaded Matrigel (Fig. 6 C). The effect of HAS2 on human lung fibroblast invasion was then investigated by knocking down gene expression using small interfering RNA (siRNA) in primary cells. We found that HAS2 suppression dramatically decreased constitutive HA production (Fig. 6 D and Fig. S4) and markedly inhibited the capacity to invade matrix (Fig. 6, D and E). We then

treated IPF fibroblasts with anti-CD44 antibodies that recognize human CD44 and demonstrated a marked reduction in invasive capacity (Fig. 6 F). Collectively, these data suggest that unrelenting pulmonary fibrosis is dependent on a matrix-invading fibroblast phenotype regulated by HAS2 and CD44.

HAS2 regulates fibroblast invasion by modulating CD44 and matrix metalloproteinase (MMP) expression levels

To gain additional insights into the potential mechanisms for the enhanced invasive phenotype of fibroblasts from both a mouse model of severe fibrosis as well as from patients with
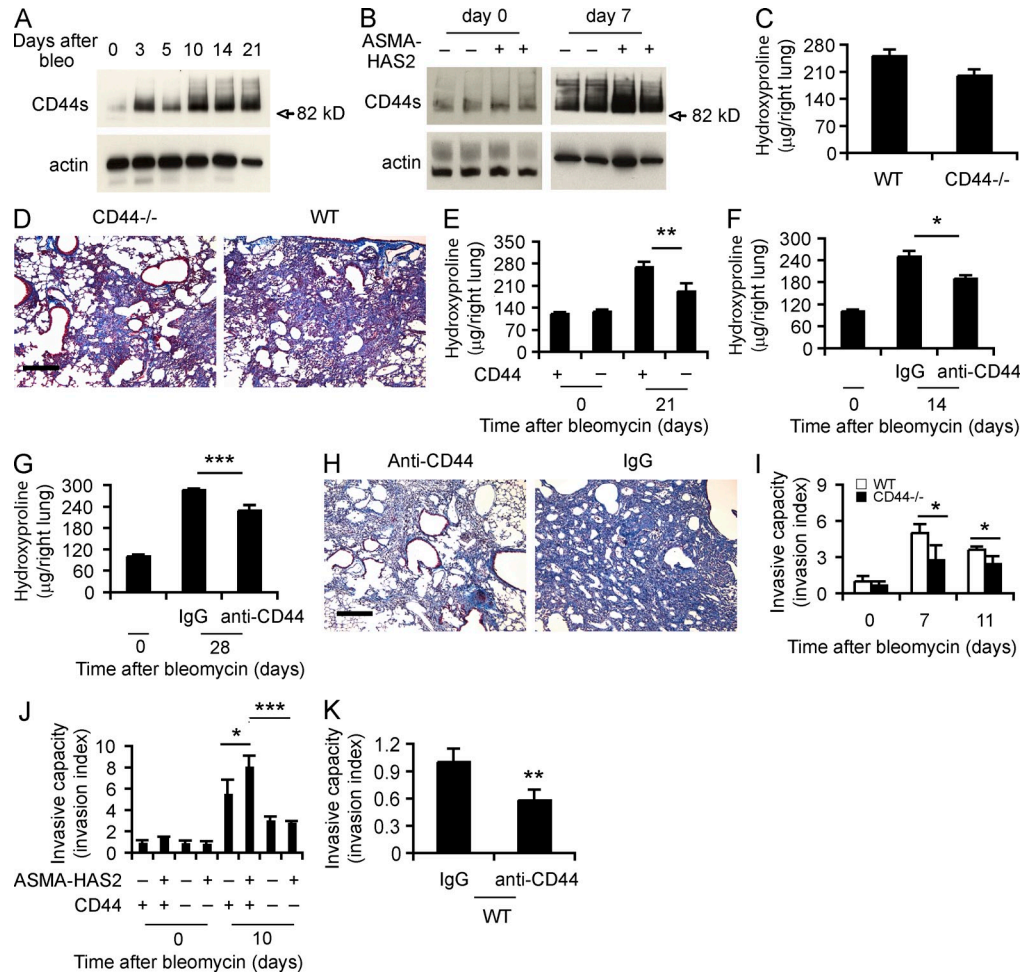
Figure 5. CD44 regulates lung fibrosis and fibroblast invasive capacity. (A) Western blot analysis of CD44 expression using KM114 anti-CD44 antibodies in WT lung tissues at the indicated times after bleomycin treatment. Samples loaded at each time point were the mixture of equal amounts of three samples collected per time point. β-Actin was used as a loading control. CD44 standard form (82.0 kD) is indicated. (B) Immunoblot of CD44 in ASMA-HAS2+ (+) and control (−) mouse lung tissues on days 0 and 7 after bleomycin treatment. (C) Lung tissues from CD44-null and WT mice on day 21 after bleomycin treatment were collected and assayed for collagen content using the hydroxyproline method ($n = 14$–17 per group). (A–C) The experiments were performed three times. (D) Lung sections of WT and CD44-null mice on day 21 after bleomycin instillation were stained using Masson's trichrome method. Representative images of the staining are shown ($n = 5$–6). The experiment was repeated twice. (E) Hydroxyproline content on days 0 and 21 after bleomycin treatment was analyzed in ASMA-HAS2+/CD44+/+ and ASMA-HAS2+/CD44−/− mice ($n = 7$–8 per group; **, $P < 0.01$). (F) Neutralizing anti-CD44 antibodies were instilled i.p. 12 h before and 5 d after bleomycin treatment in ASMA-HAS2+ mice. Lungs were analyzed for hydroxyproline content on day 14 after bleomycin instillation ($n = 5$–8 per group; *, $P < 0.05$). (G) Anti-CD44 neutralizing antibodies were instilled i.p. on days 7, 14, and 21 after bleomycin treatment, and lungs were analyzed for hydroxyproline content at day 28 ($n = 6$–9 per group; ***, $P < 0.001$). (E–G) The experiments were performed three times. (H) Lung sections of the mice described in G were stained using Masson's trichrome method. Representative images of the staining are shown. (I) The spontaneous Matrigel-invading capacity of fibroblasts from bleomycin-treated (7 and 11 d) and saline-treated WT C57BL/6J and CD44-null mouse lungs was determined. Data are shown as the index of invasion value of the fibroblasts with or without bleomycin treatment over WT fibroblasts without bleomycin challenge ($n = 4$ per group; *, $P < 0.05$). (J) Invasive capacity of mesenchymal cells from ASMA-HAS2−, ASMA-HAS2+, ASMA-HAS2−/CD44−/−, and ASMA-HAS2+/CD44−/− mouse lungs with or without bleomycin challenge was compared. Data are shown as the index of invasion value of the fibroblasts with or without bleomycin treatment over ASMA-HAS2− fibroblasts without bleomycin challenge ($n = 4$ per group; *, $P < 0.05$; ***, $P < 0.001$). (K) Invasion of bleomycin-treated WT mouse lung fibroblasts with (anti-CD44) or without (IgG) neutralizing CD44 antibody incubation ($n = 4$ per group; **, $P < 0.01$). (I–K) The experiments were repeated three times. (C, E–G, and I–K) Error bars indicate mean ± SEM. Bars, 200 µm.

IPF, we examined patterns of gene expression induced during invasion. Fibroblasts are heterogenous and only a subset are invasive, so we reasoned that clues to the mechanisms regulating invasion could be gained by studying fibroblasts after invasion. Fibroblasts from ASMA-HAS2^{+} mice were layered onto Matrigel-coated wells, RNA from the fibroblasts that invaded the matrix through to the underlying filter was isolated, and quantitative RT-PCR (qRT-PCR) array analysis was performed. Control samples were the fibroblasts that penetrated the filter in the absence of Matrigel. In addition to the up-regulation of HAS2 (Fig. 4 B) and CD44 (Fig. 7 B) expression in invasive cells, we identified a marked up-regulation in the expression of MMPs (MMP9, -12, and -14; Fig. 7 A), which promote fibroblast migration and invasion (Stamenkovic, 2000; Kessenbrock et al., 2010), down-regulation of tissue inhibitor of metalloproteinase (TIMP; TIMP3; Fig. 7 A), which has been shown to inhibit cell invasion of matrix (Baker et al., 1998; Kessenbrock et al., 2010), and ADAMTS1 (Fig. 7 A), which has been reported to play a role in renal fibrosis (Mittaz et al., 2005). Similar patterns of gene expression were also observed in invasive IPF fibroblasts, including an up-regulation in MMP9 (Fig. 7 C). We then investigated whether the alterations in gene expression were a direct consequence of *Has2*. Interestingly, we found that HAS2 knockdown directly suppressed CD44 and MMP9 gene and protein expression

(Fig. 7, D and E; and Fig. S5). Finally, we cultured fibroblasts from ASMA-HAS2^{+} and WT mice in Matrigel and found that fibroblasts from ASMA-HAS2^{+} fibroblasts secreted more pro-MMP9 than fibroblasts from control ASMA-HAS2^{−} mice (Fig. 7 F) that were enzymatically active (Fig. 7, G and H). Collectively, these data suggest that HA–CD44 interactions and up-regulation of HAS2 in the context of matrix induce the activation of a gene program that promotes an invasive fibroblast phenotype and severe fibrosis.

DISCUSSION
The mechanisms that control severe and progressive tissue fibrogenesis are incompletely understood. In this study, we interrogated the role of HA expression by myofibroblasts in the pathogenesis of pulmonary fibrosis. We generated a novel model of severe and progressive fibrosis after lung injury by targeting *Has2* expression to ASMA-expressing cells. Interstitial overexpression of HAS2 by myofibroblasts produced fatal lung fibrosis, whereas conditional knockout of HAS2 in mesenchymal cells thwarted both the development of lung fibrosis and emergence of myofibroblasts. We provide several lines of evidence in vivo supporting the concept that HA and its cognate cell surface receptor CD44 regulate lung fibrosis after lung injury. CD44 contributed to the progressive fibrotic phenotype because either crossing the ASMA-HAS2 transgenic mice with CD44 deficient mice or treatment with a blocking antibody to CD44 reduced lung fibrosis.
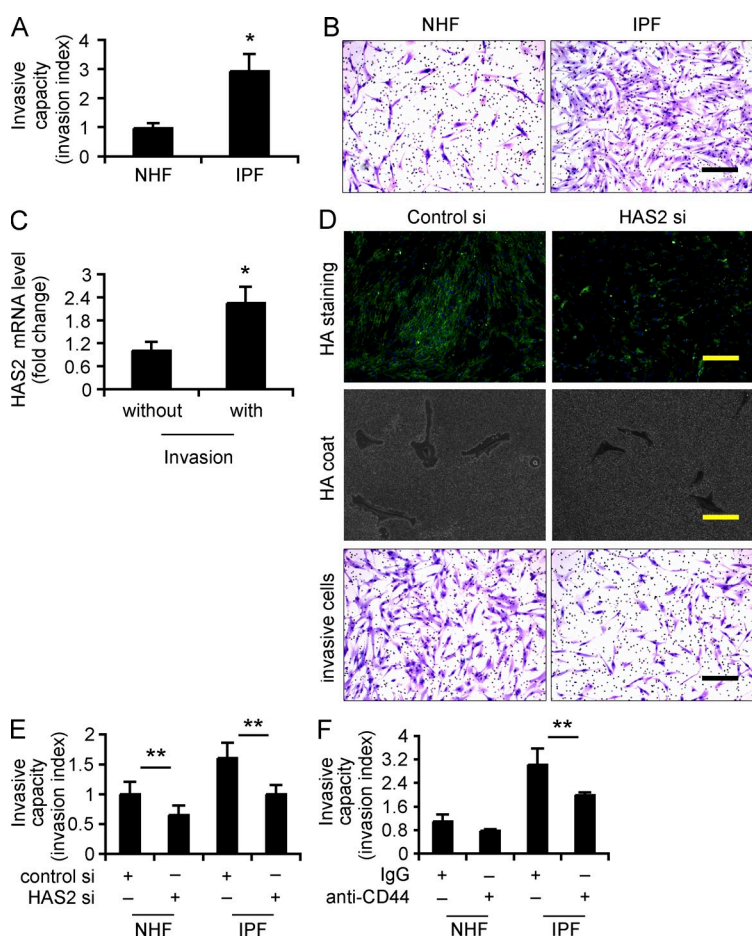

Figure 6. HAS2 and CD44 are required for human lung fibroblast invasion. (A) Invasive capacity of human fibroblasts from normal subjects (NHF; $n = 5$) and IPF patients ($n = 9$). Results are for five separate experiments and are expressed as the invasion index of the IPF fibroblasts over the normal fibroblasts (*, P < 0.05). (B) Representative images of invasive IPF fibroblasts and normal fibroblasts. (C) Relative HAS2 mRNA levels of invasive and noninvasive IPF fibroblasts were determined using real-time PCR ($n = 7$; *, P < 0.05). The experiments were repeated two times. (D) 48 h after transfection with HAS2 siRNA (HAS2 si) and control siRNA (control si), photomicrographs demonstrating the effects of HAS2 si on fibroblast cellular surface HA, photomicrographs demonstrating the effects of HAS2 si on HA coat formation, and images of invasive HAS2 siRNA– and control siRNA–transfected fibroblasts are shown. (E) 48 h after HAS2 and control siRNA transfection, equal numbers of fibroblasts from normal donors ($n = 2$) and IPF patients ($n = 3$) were loaded into invasion chambers and incubated for another 24 h. Invasive cells were counted. Data are shown as the invasion index of HAS2 siRNA–transfected normal, IPF fibroblasts and control siRNA–transfected IPF fibroblasts over control siRNA–transfected normal fibroblasts (**, P < 0.01). (F) After 20 min of incubation with anti-CD44 neutralizing or isotype-matched control IgG antibody, fibroblasts from normal donors ($n = 3$) and IPF patients ($n = 6$) were subjected to the invasion assay. Data are depicted as the invasion index (**, P < 0.01). (D–F) The experiments were repeated three times. (A, C, E, and F) Error bars indicate mean ± SEM. Bars: (B and D [top and bottom]) 200 µm; (D, middle) 100 µm.
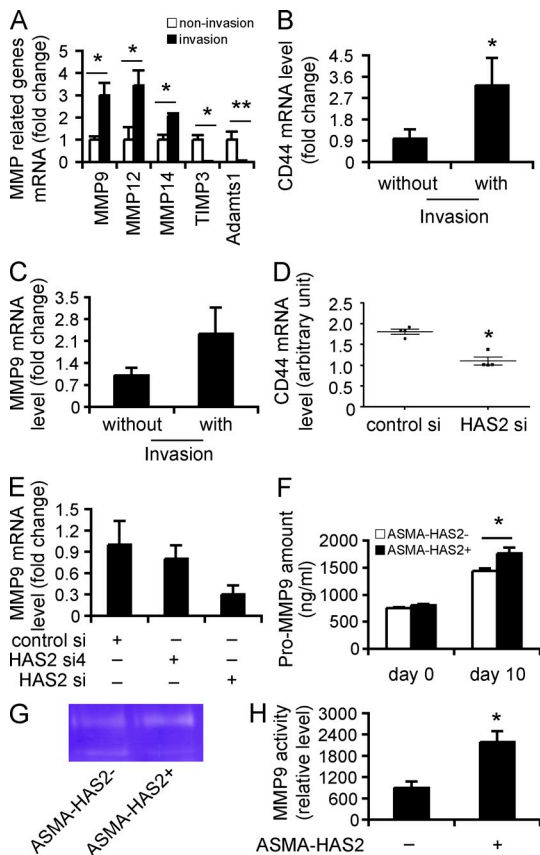
Figure 7. HAS2 promotes fibroblast invasion by regulating CD44 and MMP expression and function. (A and B) RNA was extracted from invasive ASMA-HAS2+ fibroblasts, and 84 genes were analyzed by using a specialized qRT-PCR array for extracellular matrix synthesizing and degrading enzymes. RNAs from the fibroblasts that penetrated the filter in the absence of Matrigel were used as control. Representative genes up- or down-regulated in invasive ASMA-HAS2+ fibroblasts are shown ($n = 5$; *, $P < 0.05$; **, $P < 0.01$). (B) CD44 mRNA expression in invasive fibroblasts versus noninvasive fibroblasts from bleomycin-treated ASMA-HAS2+ lungs ($n = 5$; *, $P = 0.05$). (C) MMP9 mRNA expression in invasive IPF fibroblasts was compared with IPF fibroblasts that penetrated the filters in the absence of Matrigel by using real-time PCR ($n = 5$). The experiments were performed twice. (D) CD44 mRNA expression in HAS2 siRNA (HAS2 si)–transfected fibroblasts and control siRNA (control si) transfectants was determined using a microarray assay. The horizontal bars indicate the median expression values ($n = 4$; *, $P < 0.05$). (E) 48 h after HAS2 siRNA and control siRNA transfection, fibroblasts were cultured on Matrigel for an additional 6 h. mRNA was then extracted, and MMP9 mRNA expression was measured using real-time PCR. Data shown represent one of two separate experiments. (F) Fibroblasts from ASMA-HAS2− and ASMA-HAS2+ mice were cultured on Matrigel for 96 h, and pro-MMP9 protein in the media was measured using a pro-MMP9 ELISA kit ($n = 3$–7 per group; *, $P < 0.05$). The experiments were performed three times. (G) The media described in F was concentrated 10× using Microsep centrifugal devices. Equal amounts of protein were subjected to gelatin zymography for MMP9 activity. A representative image is shown. The experiments were repeated two times. (H) Quantification analysis of gelatin zymography for MMP9 activity results by using ImageJ software ($n = 4$–5 per group; *, $P < 0.05$). (A–F and H) Error bars indicate mean ± SEM.

We provide in vivo evidence demonstrating that myofibroblasts directly contribute to exaggerated fibrosis. There are multiple studies suggesting that expression of ASMA is a hallmark of fibroblastic foci in IPF (Hinz et al., 2007; Larsson et al., 2008), and myofibroblast accumulation has been demonstrated in experimental lung fibrosis (Horowitz et al., 2007; Kim et al., 2009). Although the source of myofibroblasts in the fibrotic lung have been suggested from a variety of sources including resident fibroblasts (Hinz et al., 2007), epithelial cells (Kim et al., 2009), or bone marrow (Epperly et al., 2003; Hashimoto et al., 2004), the contribution of myofibroblasts to fibrogenesis is well accepted. It should be noted that ASMA–expressing cells also include endothelial cells (Lu et al., 2004) and bone marrow stroma (Peled et al., 1991), although the expression in these cells may require activation by TGF-β or tissue injury (Ando et al., 1999).

A salient feature of this progressive fibrotic phenotype was the acquired ability of fibroblasts/myofibroblasts to invade extracellular matrix. We confirmed previous observations that fibroblasts from patients with IPF show an invasive property when compared with fibroblasts from normal individuals (White et al., 2003a). IPF biopsies often show areas of denuded basement membrane (White et al., 2003a), possibly resulting from alveolar epithelial cell apoptosis (Kuwano et al., 2002). The destruction of basement membrane was also observed in experimental lung injury and fibrosis (Fukuda et al., 1985; Vaccaro et al., 1985). Similar to cancer cells, fibrotic myofibroblasts acquire the ability to invade damaged basement membrane underneath the epithelium. Previous studies suggest that integrins (White et al., 2003b) and urokinase-type plasminogen activator cellular receptor (Zhu et al., 2009) may have a role in fibroblast invasion during lung fibrogenesis. We demonstrated that the invasive phenotype required both HAS2 and CD44 because targeting either by multiple approaches inhibited tissue invasion. The invasive phenotype of IPF fibroblasts was abrogated by down-regulating *Has2* expression. Finally, we could inhibit invasion of IPF fibroblasts with anti-CD44 antibodies. Fibroblasts from IPF patients are known to exhibit heterogeneous biological properties (Jordana et al., 1988). We found that the invasive phenotype emerges through contact with the matrix. Normal lung fibroblasts do not invade the matrix, and only a subset of ASMA-HAS2 transgenic and IPF fibroblasts are invasive. Importantly, we are the first to show that targeting invasion is effective in ameliorating pulmonary fibrosis. Collectively, these data identify a previously unrecognized pathway by which fibrotic fibroblasts acquire an invasive phenotype analogous to metastatic cancer cells.

We propose that progressive lung fibrosis requires the generation of an activated myofibroblast phenotype that is characterized by HAS2 expression and the ability to invade basement membrane at least partly through CD44 and coordinated expression of MMPs and inhibitors of MMP functions. We provide data in support of a previously unsuspected role for myofibroblast production of HA as a downstream mediator of persistent lung fibrosis by promoting the generation

of an invasive fibroblast phenotype. These data suggest that HAS2 plays a key role in promoting fibrogenesis in several ways. First, HAS2 overexpression increased CD44 expression and HA production. Second, HAS2 overexpression promoted activation of a gene program that facilitates emergence of an invasive phenotype. We identified an up-regulation in the expression of MMPs and down-regulation of tissue inhibitors of metalloproteinase. The resultant imbalance in the ratio of MMP/TIMP expression in fibrotic fibroblasts provides a mechanism to promote tissue invasion. MMP-12 has been shown to contribute to pulmonary fibrosis in two different model systems, although the precise mechanism is unknown (Kang et al., 2007; Madala et al., 2010). The loss of Timp-3 leads to the development of kidney fibrosis (Kassiri et al., 2009). In addition, mice deficient in Timp3 have increased expression of MMP1a and enhanced pulmonary fibrosis after bleomycin treatment (Gill et al., 2010). We also observed the down-regulation of a disintegrin-like and metallopeptidase (ADAMS) with thrombospondin type 1 motif 1 (ADAMTS1). ADAMTS1 is a procollagen N-proteinase that processes several types of procollagen proteins to mature collagen and is also important for collagen fibril assembly in the extracellular matrix. ADAMTS1 has not been explored in lung fibrosis, but it has been reported to play a role in renal fibrosis (Shindo et al., 2000; Mittaz et al., 2005). Deletion of Adamts1 increased interstitial fibrosis in the kidney (Shindo et al., 2000). Given the multiple roles in tumor microenvironment, it is anticipated that MMPs (Kessenbrock et al., 2010), ADAMS (Murphy, 2008), and cell adhesion molecules coordinate with extracellular components such as HA and CD44 to regulate fibrotic fibroblast invasion. Although our experiments have focused on HAS2, we cannot exclude roles for HAS1 and HAS3.

Further studies will be required to determine whether the development of an invasive fibrotic phenotype requires growth factors such as TGF-β or PDGF (platelet-derived growth factor). TGF-β has been recognized as a critical regulator of tissue fibrosis in general, and numerous studies have provided strong support in favor of a nonredundant role in lung fibrosis in particular (Sime et al., 1997; Munger et al., 1999). TGF-β has been shown to be required for the development of bleomycin-induced pulmonary fibrosis, is a potent stimulator of HA production, and has been shown to promote the transition of resident fibroblasts to myofibroblasts in vitro (Webber et al., 2009). The downstream effector pathways following TGF-β activation leading to unrelenting tissue fibrosis have not been fully elucidated. Numerous studies suggest that TGF-β regulates the expression of MMP/TIMP balance (Kim et al., 2004; Kang et al., 2007). Furthermore, CD44 has been shown to interact with MMP-9 and promote tumor metastasis by serving as a cell surface docking receptor for proteolytically active MMP-9 that cleaves latent TGF-β to release active TGF-β during tumor metastasis (Yu and Stamenkovic, 2000). CD44 has been shown to directly interact with MMP-14 (MT1-MMP) to promote tumor cell invasion (Marrero-Diaz et al., 2009). We anticipate that progressive lung fibrosis requires the generation of an invasive myofibroblast phenotype that requires TGF-β, where HAS2 and CD44 are critical downstream components of TGF-β–induced fibrosis. Collectively, genes that are dysregulated in Has2-overexpressing myofibroblasts are important for cellular invasion on multiple fronts and may indicate another link between severe fibrosis and metastatic cancers.

Myofibroblast CD44 coupled with *Has2* overexpression promotes the emergence of a gene program essential for tissue invasion. A novel aspect of this study is the observation that the emergence of the invasive phenotype appears to require contact with the matrix. The finding that coordinated gene expression with up-regulation of matrix-degrading enzymes and down-regulation of inhibitors of these enzymes occurs in both mouse and man suggests that this approach could be used to identify therapeutic targets. The proof of principle experiments that CD44 antibodies attenuated lung fibrosis in mice in vivo encourages further investigations of this pathway. Understanding the genomic and translational programs leading to an invasive myofibroblast phenotype and elucidating the proximal signaling pathways that mediate HA and CD44 effects on fibroblast invasion could represent novel approaches to the treatment of disorders characterized by progressive tissue fibrosis.

MATERIALS AND METHODS

Mice. ASMA–human HAS2 transgenic mice (ASMA-HAS2⁺) were described previously (Chai et al., 2005). The conditional *Has2*-null allele was generated using the Cre/loxP system (Matsumoto et al., 2009). HAS2 protein is a multipass transmembrane protein. This conditional allele was designed in such a way that exon 2, which contains the start codon as well as two N-terminal transmembrane domains crucial for the insertion of HAS2 protein into the plasma membrane, is deleted upon Cre-mediated recombination, and thereby no HAS2 protein is produced. *Has2*$^{flox/+}$ designates the intact conditional allele before recombination. The Cre recombinase–expressing mice under the control of the collagen1α2 promoter and enhancer (Col1α2-iCre⁺) were provided by P. Angel (Deutsches Krebsforschungszentrum, Heidelberg, Germany; Florin et al., 2004). For the conditional deletion of HAS2, two chimeras of *Has2*$^{flox/+}$ mice were crossbred to obtain *Has2*$^{flox/flox}$ homozygous mice. *Has2*$^{flox/flox}$ homozygous mice were then crossed with Col1α2-iCre⁺ mice to generate *Col1α2-iCre⁺/Has2*$^{flox/+}$. Further breeding with *Has2*$^{flox/flox}$ homozygous mice resulted in four genotypes in the offspring, including the conditional knockout mutant for *Has2* (*Col1α2-iCre⁺/Has2*$^{−/−}$; termed *Has2*$^{CKO/CKO}$). Mice expressing Cre under the control of the FSP-1 (also called S100A4) promoter (FSP-1–Cre) were provided by T. Blackwell (Vanderbilt University, Nashville, TN; Lawson et al., 2005; Tanjore et al., 2009). CD44$^{−/−}$ mice were provided by T.W. Mak (Amgen Research Institute, Toronto, Ontario, Canada; Schmits et al., 1997). We crossbred ASMA-HAS2⁺ with CD44$^{−/−}$ to generate chimeras of ASMA-HAS2⁺/CD44$^{+/−}$, and we then backcrossed the two chimeras to get ASMA-HAS2⁺/CD44$^{−/−}$ mice. C57BL/6J mice were obtained from The Jackson Laboratory. All mice were housed in a pathogen-free facility at Duke University, and all animal experiments were approved by the Institutional Animal Care and Use Committee at Duke University.

Fibroblast isolation and culture. Primary fibroblasts were derived from mouse lungs as described previously (Tager et al., 2008; Jiang et al., 2010). The cells were used from three to six generations. Human lung fibroblasts were isolated from surgical lung biopsies or lung transplant explants obtained from patients with IPF. Normal lung fibroblasts were obtained from discarded portions of normal transplant donor lung tissue. The specimens were

obtained under the auspices of Institutional Review Board–approved protocols. The tissues were minced and cultured in DME supplemented with 15% FBS, 100 U/ml penicillin, 100 µg/ml streptomycin, 5 µg/ml gentamicin, and 0.25 µg/ml amphotericin B. The cells of passage 5–7 were used for invasion assays, siRNA interference assays, and HA coat and HA amount measurements. The diagnosis of IPF was arrived at by standard accepted American Thoracic Society recommendations (ATS/ERS, 2000). All experiments were approved by the Duke University Institutional Review Board and in accordance with the guidelines outlined by the board.

Bleomycin administration and BAL. Bleomycin was injected intratracheally at either a dose of 2.5 U/kg body weight for analysis of the early inflammatory response or 1.75 U/kg body weight for analysis of the late fibrotic response. Anesthesia was provided with a mixture of ketamine of 100 mg/kg (Fort Dodge) and xylazine of 10 mg/kg (Shenandoah). At designated time points after bleomycin injection, mice were euthanized by ketamine mixture injection, and lungs were harvested for RNA preparation, protein isolation, or fibroblast isolation. For BAL, the trachea was lavaged three times with 0.8 ml sterile saline at room temperature. Samples were centrifuged at 1,500 rpm for 5 min, and the supernatant was collected and stored at −80°C until used. The cell-free supernatants were then analyzed for HA and chemokine KC concentrations by specific ELISA. The cell pellets were resolved in 1 ml sterile saline, and the cells were counted with a hemocytometer. Approximately 40,000 cells from each specimen were loaded onto slides. These slides were stained using a Protocol Hema 3 stain set (Thermo Fisher Scientific) and reviewed under light microscopy for white blood cell differential.

HA quantification. BALF and lung tissues were collected at different times after bleomycin treatment. Lung tissues were excised, weighed, and homogenized as described previously (Teder et al., 2002). After centrifugation, the HA content in the tissue supernatants and in BALF was measured using the HA-ELISA (Teder et al., 2002). The HA content in cultured media of human lung fibroblasts was quantified using the same ELISA method.

Histology, ASMA, and HA immunohistochemistry. Three to eight mice in each group were sacrificed at various times after bleomycin treatment under anesthesia. The trachea was cannulated, and the lungs were inflated with 1 ml of 10% formalin. The tissues were then fixed overnight, embedded in paraffin, and sectioned for staining with hematoxylin and eosin or Masson's trichrome. Paraffin-embedded lung samples were also analyzed for HA localization. After being dewaxed and rehydrated, tissues were incubated with 4 µg/ml biotin-labeled HA-binding protein (HABP; Associates of Cape Cod, Inc.) for 1 h and then incubated and developed using a VECTA-STAIN Elite ABC kit (Vector Laboratories). The specificity of the staining was determined by preincubating tissue samples with 10 U/ml streptomyces hyaluronidase for 2 h at room temperature. For ASMA staining, tissue sections were incubated with horseradish peroxidase–conjugated anti-ASMA monoclonal antibody (Dako) and then incubated with the VECTASTAIN Elite ABC kit as described above. For HA and ASMA double staining, tissue sections were incubated with biotin-HABP overnight at 4°C, followed by incubation with Cy3-labeled anti-ASMA antibody (Sigma-Aldrich) to detect ASMA and streptavidin and Alexa Fluor 488 conjugate (Invitrogen) to detect HA. The processed sections were mounted in Fluoromount-G (Immunokemi) containing DAPI and photographed with a microscope (Axio Imager A1; Carl Zeiss).

Hydroxyproline assay. Collagen content in lung tissue from 4–17 mice per group was measured with the conventional hydroxyproline method (Adamson and Bowden, 1974). The ability of the assay to completely hydrolyze and recover hydroxyproline from collagen was confirmed using samples containing known amounts of purified collagen.

Quantification of mRNA expression. Real-time RT-PCR was used to quantify the relative mRNA levels of HAS2 in C57BL/6J mice with or without bleomycin instillation using gene-specific primers. In brief, total RNA was purified using RNAqueous-4PCR kit (Invitrogen) and was reversed to cDNA using SuperScript II RNase H⁻ RT kit (Invitrogen) according to the manufacturer's instructions. *HAS2* gene levels in the resultant cDNAs were examined using the ABI Prism 7500 Detection system (Applied Biosystems) with SYBR green as fluorescent dye enabling real-time detection of PCR products according to the manufacturer's protocol (Power SYBR green PCR Master Mix; Applied Biosystems). The relative expression levels of the gene were determined against *GAPDH* levels in the samples. The same method was used to measure the relative mRNA levels of mouse *HAS2* and human *HAS2* genes in ASMA-HAS2⁺ mice and transgene–negative littermate controls with or without bleomycin treatment and was used to measure HAS2, MMP9, MMP12, and MMP14 mRNA levels in mouse and human lung fibroblasts. The following primers were used: human HAS2 (GenBank/EMBL/DDBJ accession no. NM_005328) forward, 5′-TCGCAACACGTAACGCAAT-3′; human HAS2 reverse, 5′-ACTTCTCTTTTTCCACCCCATTT-3′; human MMP9 (GenBank accession no. NM_004994) forward, 5′-CCCACTGCTGGCCCTTCTA-3′; human MMP9 reverse, 5′-TCACGTTGCAGGCATCGT; human MMP12 (GenBank accession no. NM_002426) forward, 5′-TGCACGCACCTCGA-TGTG-3′; human MMP12 reverse, 5′-GGCCCCCCTGGCATT-3′; human MMP14 (GenBank accession no. NM_004995) forward, 5′-CGAGAG-GAAGGATGGCAAATT-3′; human MMP14 reverse, 5′-AGGGAC-GCCTCATCAAACAC-3′; human *GAPDH* (NM_002046) forward, 5′-CCCATGTTCGTCATGGGTGT-3′; human *GAPDH* reverse, 5′-TGGT-CATGAGTCCTTCCACGATA-3′; mouse HAS2 (GenBank accession no. NM_008216) forward, 5′-ACGACGACCTTTACATGATGGA-3′; mouse HAS2 reverse, 5′-GATGTACGTGGCCGATTTGCT-3′; mouse *GAPDH* forward, 5′-ATCATCTCCGCCCCTTCTG-3′; and mouse *GAPDH* reverse, 5′-GGTCATGAGCCCTTCCACAAC-3′.

Microarray assay. At 48 h after transfection, RNA from HAS2 siRNA– and control siRNA–transfected human lung fibroblasts was purified using the RNAqueous-4PCR kit. Affymetrix microarray (genechip U133A 2.0) was used for comparing CD44 gene expression level in the HAS2 knockdown cells with that in the control cells.

qRT-PCR array assay. Fibroblasts from bleomycin-treated ASMA-HAS2⁺ mice were loaded onto 6-well Matrigel chambers or 6-well insert chambers without Matrigel (BD) and cultured in a CO_2 incubator for 48 h. Matrigel matrix and noninvading cells on the upper surface of the filter were removed by wiping with a cotton swab, the polycarbonate filters with the invaded cells or migrated cells were washed once with PBS, and RNA was isolated from the cells using the RNAqueous-4PCR kit. RT was performed using the RT² First Strand cDNA Synthesis kit (QIAGEN), and 84 genes were assessed by RT-PCR using the Mouse Extracellular Matrix and Adhesion Molecules array (RT² Profiler PCR Array PAMM-013; QIAGEN) according to the manufacturer's instructions using the ABI Prism 7500 Detection system. For analysis, the expression level for each gene of interest (GOI) was calculated as 2-Ct followed by normalization to GAPDH (HKG), using the formula 2 − (Ct GOI − Ct HKG). Ultimately, the fold change in normalized gene expression was calculated by comparing values from the invaded fibroblasts through Matrigel (with invasion) with the migrated fibroblasts through filter without Matrigel (without invasion) according to the following formula: 2-Ct with invasion/2-Ct without invasion. Values were calculated for replicates of five independent experiments.

HA pericellular coat determination. Fibroblasts isolated from *Has2^{flox/+}*, *Has2^{CKO/CKO}* mouse lungs, and fibroblasts from human lung tissues were incubated at 10^4 cells/well of a 6-well plate for 24 h in 10% FBS-DME and were then overlaid with 10^7 erythrocytes. The erythrocytes were allowed to settle for 15 min at room temperature, and the cells were observed with an inverted microscope with a phase contrast at 200× magnification with a camera (AxioCam MRC5; Carl Zeiss). The size of the pericellular coat was defined by the subtraction between the area excluding erythrocytes and cell area by using the ImageJ program (National Institutes of Health).

Matrigel invasion assay. The invasive behavior of fibroblasts isolated from WT, ASMA-HAS2$^+$, ASMA-HAS2$^-$, *Has2*$^{CKO/CKO}$, *Has2*$^{FKO/FKO}$, ASMA-HAS2$^-$/CD44$^{-/-}$, ASMA-HAS2$^+$/CD44$^{-/-}$, and CD44$^{-/-}$ mouse lungs was performed essentially as described previously (Li et al., 2007; Hager et al., 2009). Equal numbers of fibroblasts were plated onto the BioCoat Matrigel Invasion Chamber (BD), and the cell invasion was performed in the presence of 10% FBS complete medium. After 24 h of incubation in a CO_2 incubator, media were removed, and the polycarbonate filters with the invaded cells were washed once with PBS followed by fixing and staining with the Protocol Hema 3 stain set. Matrigel matrix and noninvading cells on the upper surface of the filter were removed by wiping with a cotton swab, and the filters were removed from the insert by a scalpel blade and were mounted onto glass slides. The invading cells of each sample were counted in five randomly selected fields of duplicate filters under a microscope at 400× magnification. The invasive capacity of fibroblasts from IPF patients was compared with fibroblasts from normal donors using the same invasion assay. CD44 effects on mouse and human lung fibroblasts invasion were assessed using 15 µg/ml anti-CD44 blocking antibodies (5F12 clone for human CD44; KM201 for mouse CD44). The cells were incubated with anti-CD44 or isotype-matched IgG for 20 min before performing the invasion assay. The effects of HAS2 expression levels on human lung fibroblasts' invasion were investigated by performing the invasion assay at 48 h after HAS2 siRNA and control siRNA transfection.

RNA interference assay. Four siRNA duplexes designed to target different nucleotide sequences (HAS2 si, 1530–1550; HAS2 si2, 1051–1071; HAS2 si3, 1424–1444; and HAS2 si4, 1777–1797) of the human HAS2 gene (GenBank accession no. NM_005328) were obtained from QIAGEN. Subconfluent fibroblasts (~50–60% confluent) grown in complete medium were transfected separately with each one of the four siRNA duplexes or with a control siRNA (control si; QIAGEN) at the concentration of 100 nM using Hiper-Fect transfection reagent (QIAGEN) according to the manufacturer's instructions. The suppression efficiency of each one of the four siRNA duplexes was examined by measuring the HA content in the conditioned culture media after 48 and 72 h of transfection, HAS2 mRNA at 72 h after transfection, and HA coat at 48 h after transfection. The HAS2 siRNA corresponding to nucleotide sequences 1530–1550 of the HAS2 cDNA (5′-CAGCTCGATC-TAAGTGCCTTA-3′; HAS2 si) was used for all experiments.

Western blotting. WT, ASMA-HAS2$^+$, and littermate control lung tissues after bleomycin treatment were homogenized in radioimmunoprecipitation assay buffer. The proteins were fractionated by SDS-PAGE using gradient gel (4–20%; Bio-Rad Laboratories) and electroblotted onto nitrocellulose membrane (Bio-Rad Laboratories). The membranes were probed with a rat monoclonal anti-CD44 antibody (KM114; BD) and then probed with relative second antibody. β-Actin was used as a loading control.

Administration of neutralizing anti-CD44 monoclonal antibody. TIB-240 hybridoma cells producing rat anti–mouse CD44 blocking antibody (KM201) were purchased from the American Type Culture Collection. The antibody was isolated using saturated ammonium sulfate method. Two schemes were used for the antibody administration. For the preventive protocol, KM201 or isotype control rat IgG$_1$ (300 µg in 500 µl saline) was administered i.p. 12 h before bleomycin challenge, and repeated injections were given in the same way (200 µg/500 µl saline) on day 5 after bleomycin treatment. 14 d after bleomycin challenge, mouse lungs were collected, and collagen content in the mouse lungs was measured using the hydroxyproline assay (Adamson and Bowden, 1974). For the therapeutic protocol, KM201 or isotype control rat IgG$_1$ (300 µg in 500 µl saline) was administered i.p. at day 7 after bleomycin treatment, and repeated injections were given in the same way at days 14 and 21 after bleomycin treatment. 28 d after bleomycin challenge, mouse lungs were collected, and collagen content in the mouse lungs was measured using hydroxyproline (Adamson and Bowden, 1974).

Statistical analysis. Data are expressed as the mean ± SEM where applicable. We assessed differences in measured variables using the unpaired two-sided Student's t test or Wilcoxon rank-sum test with nonparametric data. Differences between multiple groups were calculated using one-way analysis of variance with Tukey-Kramer posttest or two-way analysis of variance with Bonferroni multiple comparisons. Statistic significance of survival curves was analyzed with the log-rank test. Statistical difference was accepted at $P < 0.05$. Prism 5.0 (GraphPad Software) or JMP5 software (SAS Institute) was used to perform statistical analysis.

Online supplemental material. Fig. S1 shows that ASMA-HAS2$^+$ mice exhibit an increase in neutrophil recruitment after lung injury. Fig. S2 shows increased HA fragment accumulation in ASMA-HAS2$^+$ mouse lungs after bleomycin treatment. Fig. S3 shows that targeted deletion of HAS2 in mesenchymal cells inhibits lung fibrosis and myofibroblast accumulation. Fig. S4 shows that *HAS2* siRNA efficiently reduces HAS2 gene expression and HA production in primary human lung fibroblasts. Fig. S5 shows that suppression of HAS2 decreased CD44 protein level. Online supplemental material is available at http://www.jem.org/cgi/content/full/jem.20102510/DC1.

REFERENCES

Acharya, P.S., S. Majumdar, M. Jacob, J. Hayden, P. Mrass, W. Weninger, R.K. Assoian, and E. Puré. 2008. Fibroblast migration is mediated by CD44-dependent TGF beta activation. *J. Cell Sci.* 121:1393–1402. doi:10.1242/jcs.021683

Adamson, I.Y., and D.H. Bowden. 1974. The pathogenesis of bleomycin-induced pulmonary fibrosis in mice. *Am. J. Pathol.* 77:185–197.

Ando, H., T. Kubin, W. Schaper, and J. Schaper. 1999. Cardiac microvascular endothelial cells express alpha-smooth muscle actin and show low NOS III activity. *Am. J. Physiol.* 276:H1755–H1768.

Arch, R., K. Wirth, M. Hofmann, H. Ponta, S. Matzku, P. Herrlich, and M. Zöller. 1992. Participation in normal immune responses of a metastasis-inducing splice variant of CD44. *Science.* 257:682–685. doi:10.1126/science.1496383

ATS/ERS. 2000. American Thoracic Society. Idiopathic pulmonary fibrosis: diagnosis and treatment. International consensus statement. American Thoracic Society (ATS), and the European Respiratory Society (ERS). *Am. J. Respir. Crit. Care Med.* 161:646–664.

Baker, A.H., A.B. Zaltsman, S.J. George, and A.C. Newby. 1998. Divergent effects of tissue inhibitor of metalloproteinase-1, -2, or -3 overexpression on rat vascular smooth muscle cell invasion, proliferation, and death in vitro. TIMP-3 promotes apoptosis. *J. Clin. Invest.* 101:1478–1487. doi:10.1172/JCI1584

Bjermer, L., R. Lundgren, and R. Hällgren. 1989. Hyaluronan and type III procollagen peptide concentrations in bronchoalveolar lavage fluid in idiopathic pulmonary fibrosis. *Thorax.* 44:126–131. doi:10.1136/thx.44.2.126

Bjoraker, J.A., J.H. Ryu, M.K. Edwin, J.L. Myers, H.D. Tazelaar, D.R. Schroeder, and K.P. Offord. 1998. Prognostic significance of histopathologic subsets in idiopathic pulmonary fibrosis. *Am. J. Respir. Crit. Care Med.* 157:199–203.

Blankesteijn, W.M., Y.P. Essers-Janssen, M.J. Verluyten, M.J. Daemen, and J.F. Smits. 1997. A homologue of *Drosophila* tissue polarity gene frizzled is expressed in migrating myofibroblasts in the infarcted rat heart. *Nat. Med.* 3:541–544. doi:10.1038/nm0597-541

Camenisch, T.D., A.P. Spicer, T. Brehm-Gibson, J. Biesterfeldt, M.L. Augustine, A. Calabro Jr., S. Kubalak, S.E. Klewer, and J.A. McDonald. 2000. Disruption of hyaluronan synthase-2 abrogates normal cardiac morphogenesis and hyaluronan-mediated transformation of epithelium to mesenchyme. *J. Clin. Invest.* 106:349–360. doi:10.1172/JCI10272

Chai, S., Q. Chai, C.C. Danielsen, P. Hjorth, J.R. Nyengaard, T. Ledet, Y. Yamaguchi, L.M. Rasmussen, and L. Wogensen. 2005. Overexpression of

hyaluronan in the tunica media promotes the development of atherosclerosis. *Circ. Res.* 96:583–591. doi:10.1161/01.RES.0000158963.37132.8b

DeGrendele, H.C., P. Estess, and M.H. Siegelman. 1997. Requirement for CD44 in activated T cell extravasation into an inflammatory site. *Science.* 278:672–675. doi:10.1126/science.278.5338.672

Epperly, M.W., H. Guo, J.E. Gretton, and J.S. Greenberger. 2003. Bone marrow origin of myofibroblasts in irradiation pulmonary fibrosis. *Am. J. Respir. Cell Mol. Biol.* 29:213–224. doi:10.1165/rcmb.2002-0069OC

Florin, L., H. Alter, H.J. Gröne, A. Szabowski, G. Schütz, and P. Angel. 2004. Cre recombinase-mediated gene targeting of mesenchymal cells. *Genesis.* 38:139–144. doi:10.1002/gene.20004

Fukuda, Y., V.J. Ferrans, C.I. Schoenberger, S.I. Rennard, and R.G. Crystal. 1985. Patterns of pulmonary structural remodeling after experimental paraquat toxicity. The morphogenesis of intraalveolar fibrosis. *Am. J. Pathol.* 118:452–475.

Gill, S.E., I. Huizar, E.M. Bench, S.W. Sussman, Y. Wang, R. Khokha, and W.C. Parks. 2010. Tissue inhibitor of metalloproteinases 3 regulates resolution of inflammation following acute lung injury. *Am. J. Pathol.* 176:64–73. doi:10.2353/ajpath.2010.090158

Hager, J.H., D.B. Ulanet, L. Hennighausen, and D. Hanahan. 2009. Genetic ablation of Bcl-x attenuates invasiveness without affecting apoptosis or tumor growth in a mouse model of pancreatic neuroendocrine cancer. *PLoS ONE.* 4:e4455. doi:10.1371/journal.pone.0004455

Hashimoto, N., H. Jin, T. Liu, S.W. Chensue, and S.H. Phan. 2004. Bone marrow-derived progenitor cells in pulmonary fibrosis. *J. Clin. Invest.* 113:243–252.

Hinz, B., S.H. Phan, V.J. Thannickal, A. Galli, M.L. Bochaton-Piallat, and G. Gabbiani. 2007. The myofibroblast: one function, multiple origins. *Am. J. Pathol.* 170:1807–1816. doi:10.2353/ajpath.2007.070112

Horowitz, J.C., D.S. Rogers, V. Sharma, R. Vittal, E.S. White, Z. Cui, and V.J. Thannickal. 2007. Combinatorial activation of FAK and AKT by transforming growth factor-beta1 confers an anoikis-resistant phenotype to myofibroblasts. *Cell. Signal.* 19:761–771. doi:10.1016/j.cellsig.2006.10.001

Itano, N., T. Sawai, M. Yoshida, P. Lenas, Y. Yamada, M. Imagawa, T. Shinomura, M. Hamaguchi, Y. Yoshida, Y. Ohnuki, et al. 1999. Three isoforms of mammalian hyaluronan synthases have distinct enzymatic properties. *J. Biol. Chem.* 274:25085–25092. doi:10.1074/jbc.274.35.25085

Jiang, D., J. Liang, J. Fan, S. Yu, S. Chen, Y. Luo, G.D. Prestwich, M.M. Mascarenhas, H.G. Garg, D.A. Quinn, et al. 2005. Regulation of lung injury and repair by Toll-like receptors and hyaluronan. *Nat. Med.* 11:1173–1179. doi:10.1038/nm1315

Jiang, D., J. Liang, G.S. Campanella, R. Guo, S. Yu, T. Xie, N. Liu, Y. Jung, R. Homer, E.B. Meltzer, et al. 2010. Inhibition of pulmonary fibrosis in mice by CXCL10 requires glycosaminoglycan binding and syndecan-4. *J. Clin. Invest.* 120:2049–2057. doi:10.1172/JCI38644

Jiang, D., J. Liang, and P.W. Noble. 2011. Hyaluronan as an immune regulator in human diseases. *Physiol. Rev.* 91:221–264. doi:10.1152/physrev.00052.2009

Jordana, M., J. Schulman, C. McSharry, L.B. Irving, M.T. Newhouse, G. Jordana, and J. Gauldie. 1988. Heterogeneous proliferative characteristics of human adult lung fibroblast lines and clonally derived fibroblasts from control and fibrotic tissue. *Am. Rev. Respir. Dis.* 137:579–584.

Kang, H.R., S.J. Cho, C.G. Lee, R.J. Homer, and J.A. Elias. 2007. Transforming growth factor (TGF)-beta1 stimulates pulmonary fibrosis and inflammation via a Bax-dependent, bid-activated pathway that involves matrix metalloproteinase-12. *J. Biol. Chem.* 282:7723–7732. doi:10.1074/jbc.M610764200

Karnoub, A.E., A.B. Dash, A.P. Vo, A. Sullivan, M.W. Brooks, G.W. Bell, A.L. Richardson, K. Polyak, R. Tubo, and R.A. Weinberg. 2007. Mesenchymal stem cells within tumour stroma promote breast cancer metastasis. *Nature.* 449:557–563. doi:10.1038/nature06188

Kassiri, Z., G.Y. Oudit, V. Kandalam, A. Awad, X. Wang, X. Ziou, N. Maeda, A.M. Herzenberg, and J.W. Scholey. 2009. Loss of TIMP3 enhances interstitial nephritis and fibrosis. *J. Am. Soc. Nephrol.* 20:1223–1235. doi:10.1681/ASN.2008050492

Kessenbrock, K., V. Plaks, and Z. Werb. 2010. Matrix metalloproteinases: regulators of the tumor microenvironment. *Cell.* 141:52–67. doi:10.1016/j.cell.2010.03.015

Kim, H.S., T. Shang, Z. Chen, S.C. Pflugfelder, and D.Q. Li. 2004. TGF-beta1 stimulates production of gelatinase (MMP-9), collagenases (MMP-1, -13) and stromelysins (MMP-3, -10, -11) by human corneal epithelial cells. *Exp. Eye Res.* 79:263–274. doi:10.1016/j.exer.2004.05.003

Kim, K.K., Y. Wei, C. Szekeres, M.C. Kugler, P.J. Wolters, M.L. Hill, J.A. Frank, A.N. Brumwell, S.E. Wheeler, J.A. Kreidberg, and H.A. Chapman. 2009. Epithelial cell alpha3beta1 integrin links beta-catenin and Smad signaling to promote myofibroblast formation and pulmonary fibrosis. *J. Clin. Invest.* 119:213–224.

Kuwano, K., N. Hagimoto, T. Maeyama, M. Fujita, M. Yoshimi, I. Inoshima, N. Nakashima, N. Hamada, K. Watanabe, and N. Hara. 2002. Mitochondria-mediated apoptosis of lung epithelial cells in idiopathic interstitial pneumonias. *Lab. Invest.* 82:1695–1706.

Larsson, O., D. Diebold, D. Fan, M. Peterson, R.S. Nho, P.B. Bitterman, and C.A. Henke. 2008. Fibrotic myofibroblasts manifest genome-wide derangements of translational control. *PLoS ONE.* 3:e3220. doi:10.1371/journal.pone.0003220

Lawson, W.E., V.V. Polosukhin, O. Zoia, G.T. Stathopoulos, W. Han, D. Plieth, J.E. Loyd, E.G. Neilson, and T.S. Blackwell. 2005. Characterization of fibroblast-specific protein 1 in pulmonary fibrosis. *Am. J. Respir. Crit. Care Med.* 171:899–907. doi:10.1164/rccm.200311-1535OC

Lesley, J., R. Hyman, and P.W. Kincade. 1993. CD44 and its interaction with extracellular matrix. *Adv. Immunol.* 54:271–335. doi:10.1016/S0065-2776(08)60537-4

Li, Y., L. Li, T.J. Brown, and P. Heldin. 2007. Silencing of hyaluronan synthase 2 suppresses the malignant phenotype of invasive breast cancer cells. *Int. J. Cancer.* 120:2557–2567. doi:10.1002/ijc.22550

Lu, X., J. Dunn, A.M. Dickinson, J.I. Gillespie, and S.V. Baudouin. 2004. Smooth muscle alpha-actin expression in endothelial cells derived from CD34+ human cord blood cells. *Stem Cells Dev.* 13:521–527.

Madala, S.K., J.T. Pesce, T.R. Ramalingam, M.S. Wilson, S. Minnicozzi, A.W. Cheever, R.W. Thompson, M.M. Mentink-Kane, and T.A. Wynn. 2010. Matrix metalloproteinase 12-deficiency augments extracellular matrix degrading metalloproteinases and attenuates IL-13-dependent fibrosis. *J. Immunol.* 184:3955–3963. doi:10.4049/jimmunol.0903008

Marrero-Diaz, R., J.J. Bravo-Cordero, D. Megías, M.A. García, R.A. Bartolomé, J. Teixido, and M.C. Montoya. 2009. Polarized MT1-MMP-CD44 interaction and CD44 cleavage during cell retraction reveal an essential role for MT1-MMP in CD44-mediated invasion. *Cell Motil. Cytoskeleton.* 66:48–61. doi:10.1002/cm.20325

Matsumoto, K., Y. Li, C. Jakuba, Y. Sugiyama, T. Sayo, M. Okuno, C.N. Dealy, B.P. Toole, J. Takeda, Y. Yamaguchi, and R.A. Kosher. 2009. Conditional inactivation of Has2 reveals a crucial role for hyaluronan in skeletal growth, patterning, chondrocyte maturation and joint formation in the developing limb. *Development.* 136:2825–2835. doi:10.1242/dev.038505

McKee, C.M., M.B. Penno, M. Cowman, M.D. Burdick, R.M. Strieter, C. Bao, and P.W. Noble. 1996. Hyaluronan (HA) fragments induce chemokine gene expression in alveolar macrophages. The role of HA size and CD44. *J. Clin. Invest.* 98:2403–2413. doi:10.1172/JCI119054

Mikecz, K., F.R. Brennan, J.H. Kim, and T.T. Glant. 1995. Anti-CD44 treatment abrogates tissue oedema and leukocyte infiltration in murine arthritis. *Nat. Med.* 1:558–563. doi:10.1038/nm0695-558

Mittaz, L., S. Ricardo, G. Martinez, I. Kola, D.J. Kelly, M.H. Little, P.J. Hertzog, and M.A. Pritchard. 2005. Neonatal calyceal dilation and renal fibrosis resulting from loss of Adamts-1 in mouse kidney is due to a developmental dysgenesis. *Nephrol. Dial. Transplant.* 20:419–423. doi:10.1093/ndt/gfh603

Miyake, K., C.B. Underhill, J. Lesley, and P.W. Kincade. 1990. Hyaluronate can function as a cell adhesion molecule and CD44 participates in hyaluronate recognition. *J. Exp. Med.* 172:69–75. doi:10.1084/jem.172.1.69

Munger, J.S., X. Huang, H. Kawakatsu, M.J. Griffiths, S.L. Dalton, J. Wu, J.F. Pittet, N. Kaminski, C. Garat, M.A. Matthay, et al. 1999. The integrin alpha v beta 6 binds and activates latent TGF beta 1: a mechanism for regulating pulmonary inflammation and fibrosis. *Cell.* 96:319–328. doi:10.1016/S0092-8674(00)80545-0

Murphy, G. 2008. The ADAMs: signalling scissors in the tumour microenvironment. *Nat. Rev. Cancer.* 8:932–941. doi:10.1038/nrc2459

Noble, P.W., F.R. Lake, P.M. Henson, and D.W. Riches. 1993. Hyaluronate activation of CD44 induces insulin-like growth factor-1 expression by

Matrix regulates fibroblast invasion | Li et al.

a tumor necrosis factor-alpha-dependent mechanism in murine macrophages. *J. Clin. Invest*. 91:2368–2377. doi:10.1172/JCI116469

Peled, A., D. Zipori, O. Abramsky, H. Ovadia, and E. Shezen. 1991. Expression of alpha-smooth muscle actin in murine bone marrow stromal cells. *Blood*. 78:304–309.

Qian, F., D.L. Vaux, and I.L. Weissman. 1994. Expression of the integrin alpha 4 beta 1 on melanoma cells can inhibit the invasive stage of metastasis formation. *Cell*. 77:335–347. doi:10.1016/0092-8674(94)90149-X

Schmits, R., J. Filmus, N. Gerwin, G. Senaldi, F. Kiefer, T. Kundig, A. Wakeham, A. Shahinian, C. Catzavelos, J. Rak, et al. 1997. CD44 regulates hematopoietic progenitor distribution, granuloma formation, and tumorigenicity. *Blood*. 90:2217–2233.

Selman, M., and A. Pardo. 2002. Idiopathic pulmonary fibrosis: an epithelial/fibroblastic cross-talk disorder. *Respir. Res.* 3:3. doi:10.1186/rr175

Shindo, T., H. Kurihara, K. Kuno, H. Yokoyama, T. Wada, Y. Kurihara, T. Imai, Y. Wang, M. Ogata, H. Nishimatsu, et al. 2000. ADAMTS-1: a metalloproteinase-disintegrin essential for normal growth, fertility, and organ morphology and function. *J. Clin. Invest*. 105:1345–1352. doi:10.1172/JCI8635

Siegelman, M.H., H.C. DeGrendele, and P. Estess. 1999. Activation and interaction of CD44 and hyaluronan in immunological systems. *J. Leukoc. Biol*. 66:315–321.

Sime, P.J., Z. Xing, F.L. Graham, K.G. Csaky, and J. Gauldie. 1997. Adenovector-mediated gene transfer of active transforming growth factor-beta1 induces prolonged severe fibrosis in rat lung. *J. Clin. Invest*. 100:768–776. doi:10.1172/JCI119590

Spicer, A.P., M.L. Augustine, and J.A. McDonald. 1996. Molecular cloning and characterization of a putative mouse hyaluronan synthase. *J. Biol. Chem*. 271:23400–23406. doi:10.1074/jbc.271.38.23400

Stamenkovic, I. 2000. Matrix metalloproteinases in tumor invasion and metastasis. *Semin. Cancer Biol*. 10:415–433. doi:10.1006/scbi.2000.0379

Tager, A.M., P. LaCamera, B.S. Shea, G.S. Campanella, M. Selman, Z. Zhao, V. Polosukhin, J. Wain, B.A. Karimi-Shah, N.D. Kim, et al. 2008. The lysophosphatidic acid receptor LPA1 links pulmonary fibrosis to lung injury by mediating fibroblast recruitment and vascular leak. *Nat. Med*. 14:45–54. doi:10.1038/nm1685

Tanjore, H., X.C. Xu, V.V. Polosukhin, A.L. Degryse, B. Li, W. Han, T.P. Sherrill, D. Plieth, E.G. Neilson, T.S. Blackwell, and W.E. Lawson. 2009. Contribution of epithelial-derived fibroblasts to bleomycin-induced lung fibrosis. *Am. J. Respir. Crit. Care Med*. 180:657–665. doi:10.1164/rccm.200903-0322OC

Teder, P., R.W. Vandivier, D. Jiang, J. Liang, L. Cohn, E. Puré, P.M. Henson, and P.W. Noble. 2002. Resolution of lung inflammation by CD44. *Science*. 296:155–158. doi:10.1126/science.1069659

Thannickal, V.J., D.Y. Lee, E.S. White, Z. Cui, J.M. Larios, R. Chacon, J.C. Horowitz, R.M. Day, and P.E. Thomas. 2003. Myofibroblast differentiation by transforming growth factor-beta1 is dependent on cell adhesion and integrin signaling via focal adhesion kinase. *J. Biol. Chem*. 278:12384–12389. doi:10.1074/jbc.M208544200

Toole, B.P. 2004. Hyaluronan: from extracellular glue to pericellular cue. *Nat. Rev. Cancer*. 4:528–539. doi:10.1038/nrc1391

Vaccaro, C.A., J.S. Brody, and G.L. Snider. 1985. Alveolar wall basement membranes in bleomycin-induced pulmonary fibrosis. *Am. Rev. Respir. Dis.* 132:905–912.

Webber, J., S. Meran, R. Steadman, and A. Phillips. 2009. Hyaluronan orchestrates transforming growth factor-beta1-dependent maintenance of myofibroblast phenotype. *J. Biol. Chem.* 284:9083–9092. doi:10.1074/jbc.M806989200

White, E.S., M.H. Lazar, and V.J. Thannickal. 2003a. Pathogenetic mechanisms in usual interstitial pneumonia/idiopathic pulmonary fibrosis. *J. Pathol*. 201:343–354. doi:10.1002/path.1446

White, E.S., V.J. Thannickal, S.L. Carskadon, E.G. Dickie, D.L. Livant, S. Markwart, G.B. Toews, and D.A. Arenberg. 2003b. Integrin alpha4beta1 regulates migration across basement membranes by lung fibroblasts: a role for phosphatase and tensin homologue deleted on chromosome 10. *Am. J. Respir. Crit. Care Med*. 168:436–442. doi:10.1164/rccm.200301-041OC

Yu, Q., and I. Stamenkovic. 2000. Cell surface-localized matrix metalloproteinase-9 proteolytically activates TGF-beta and promotes tumor invasion and angiogenesis. *Genes Dev*. 14:163–176.

Zhang, H.Y., M. Gharaee-Kermani, K. Zhang, S. Karmiol, and S.H. Phan. 1996. Lung fibroblast alpha-smooth muscle actin expression and contractile phenotype in bleomycin-induced pulmonary fibrosis. *Am. J. Pathol*. 148:527–537.

Zhu, S., C.L. Gladson, K.E. White, Q. Ding, J. Stewart Jr., T.H. Jin, H.A. Chapman Jr., and M.A. Olman. 2009. Urokinase receptor mediates lung fibroblast attachment and migration toward provisional matrix proteins through interaction with multiple integrins. *Am. J. Physiol. Lung Cell. Mol. Physiol*. 297:L97–L108. doi:10.1152/ajplung.90283.2008